coatings

MDPI

Article

Study of a Particle Based Films Cure Process by High-Frequency Eddy Current Spectroscopy

Iryna Patsora [1,*], Henning Heuer [1,2], Susanne Hillmann [2] and Dmytro Tatarchuk [3]

1 The Institute of Electronic Packaging Technology, Faculty of Electrical and Computer Engineering, Technische Universität Dresden, Mommsenstrasse 15, Dresden 01069, Germany; henning.heuer@ikts.fraunhofer.de

2 Fraunhofer Institute for Ceramic Technologies and Systems, Maria-Reiche Str. 22, Dresden 01109, Germany; susanne.hillmann@ikts.fraunhofer.de

3 Microelectronics Department, Faculty of Electronics, National Technical University of Ukraine "Igor Sikorsky Kyiv Polytechnic Institute", Peremohy Ave 37, Kyiv 03056, Ukraine; dmitry.tatarchuk@gmail.com

* Correspondence: patsyora@avt.et.tu-dresden.de; Tel.: +49-351-463-33007

Academic Editor: Günter Motz
Received: 21 September 2016; Accepted: 19 December 2016; Published: 28 December 2016

Abstract: Particle-based films are today an important part of various designs and they are implemented in structures as conductive parts, i.e., conductive paste printing in the manufacture of Li-ion batteries, solar cells or resistive paste printing in IC. Recently, particle based films were also implemented in the 3D printing technique, and are particularly important for use in aircraft, wind power, and the automotive industry when incorporated onto the surface of composite structures for protection against damages caused by a lightning strike. A crucial issue for the lightning protection area is to realize films with high homogeneity of electrical resistance where an in-situ noninvasive method has to be elaborated for quality monitoring to avoid undesirable financial and time costs. In this work the drying process of particle based films was investigated by high-frequency eddy current (HFEC) spectroscopy in order to work out an automated in-situ quality monitoring method with a focus on the electrical resistance of the films. Different types of particle based films deposited on dielectric and carbon fiber reinforced plastic substrates were investigated in the present study and results show that the HFEC method offers a good opportunity to monitor the overall drying process of particle based films. Based on that, an algorithm was developed, allowing prediction of the final electrical resistance of the particle based films throughout the drying process, and was successfully implemented in a prototype system based on the EddyCus® HFEC device platform presented in this work. This prototype is the first solution for a portable system allowing HFEC measurement on huge and uneven surfaces.

Keywords: EddyCus®; eddy wet; eddy current; HFEC; particle based films; in-situ quality control; noninvasive method; composite material; drying process

1. Introduction

Particle based films mean alternative coatings, consisting of a carrying matrix, different filler material, e.g., conductive particles, fibers, nanotubes, and nanoparticles, etc., which are distributed in a matrix by adding additional solvents [1–5]. The functional purpose of the particle based films defines the physical and mechanical properties they should possess and determines a suitable method for their application to the desired surface e.g., printing, spraying, and spin-coating techniques [6] as well as physical vapor deposition (PVD) [7], resin transfer molding (RTM) [8] and other molding methods (e.g., compression, vacuum, resin injection) [9], etc.

According to the diversity of the application method and the distinguishing feature of particle based films to combine properties from both filler material and carrying matrix [10,11] they have been successfully implemented in industry and are presently an important part of various designs. They are applied for example by conductive paste printing in integrated circuits, manufacturing of Li-ion batteries or solar cells [12]. Recently particle based films were also used in the 3D printing technique [13]. Particularly important are particle based films for aircraft, wind power and the automotive industry being incorporated onto the surface of composite structures, e.g., carbon or glass fiber reinforced plastics (CFRP and GFRP), for protection against damage caused by a lightning strike [11,14]. This application area is principally the focus of our attention in this work.

When particle based films are used as a protection surface layer deposited onto composite structures in aircraft etc. it is very important that the electrical resistance of the films stays homogeneous in the coated area to avoid critical local current densities [4–18]. This homogeneity defines the films quality. It is important to note that in aircraft and wind power industries big and convoluted shapes have to be coated by particle based films. Thus, it is either impossible to use some of the application methods (e.g., spin-coating) or the cost is high when applying films by high precision application techniques (PVD, RTM, etc.). Therefore, spraying or printing methods are more suitable for this purpose. In either case, defects in the films homogeneity can occur during their manufacturing and application, that can only be detected after the films curing process is finished, leading to undesirable financial and time costs. Therefore, an in-situ fast monitoring method is needed to provide an opportunity to predict the particle based films electrical resistance in a wet state whilst allowing adjustments.

According to the literature, many studies have been focused on finding inspection and monitoring methods for quality assurance of particle based films. Thus, in [19] and in [20] authors reported the successful application of terahertz conductivity measurements to monitor thin films with different filler content. However, this method is suitable for ultra-thin films with a thickness well below the skin depth. Hence, the method is not applicable for lightning protection films having a thickness in the micrometer range [16]. Another work of Zhang [20] illustrated application of the X-ray method to study the structure formation process of nanoparticle thin films. However, the method is more useful for stationary measurements and not for convoluted shapes requiring a quick-working portable method and also is expensive. The work by author Eslamian Morteza [12] showed the study of the dynamics of the spray coating process by using microscope videos. However, in the case of optical methods, it is possible to detect defects only on the top of the layer and seems not to be suitable for films having a thickness higher than one micrometer. Moreover, only visual defects can be controlled by the method and not the conductivity of the film.

This work aimed to investigate the drying process of particle based films by monitoring their electrical resistance using a non-destructive HFEC spectroscopy, that works quickly, is noninvasive and therefore can be applied to wet as well as to dried films; working in a high-frequency range, it reacts to the smallest changes in electrical and dielectric properties of the particle based films [5]. Furthermore, based on HFEC a portable measuring system can be developed to monitor the in-situ films drying process on big and convoluted shapes.

In order to validate the HFEC method for an in-situ monitor of particle based films electrical resistance, different types of films were produced, deposited on the dielectric substrate and CFRP and measured using the HFEC system based EddyCus® designed and manufactured by Fraunhofer IKTS (Dresden, Germany). The chemical composition of the films provided a drying process at room temperature and normal conditions, and each parameter could be varied, e.g., type of a filler, polymer matrix type or even coated area and thickness. Knowing exactly the composition of the particle based films it becomes possible to investigate the influence of different film parameters on their percolation behavior during curing in a slow drying motion mode without additional noises caused by temperature rise.

The results give an approach to monitor the films' electrical resistance beginning from films which are in a liquid state until they are dried. Based on this, an algorithm is developed, allowing prediction

of the final electrical resistance of the particle based films throughout the drying process, which makes it possible to monitor the in-situ particle based films electrical resistance. This algorithm was successfully implemented in a prototype system based on the EddyCus® HFEC device platform presented in this work. This prototype is the first solution for a portable system allowing measuring on huge and uneven surfaces.

2. Materials and Methods

2.1. HFEC

Typically, eddy current (EC) equipment consists of an electronic oscillator (i.e., generator), electronics, and a coil or combination of a coil to give a transmitting and a pickup coil. The signal from the receiving coil is analyzed, which is influenced by the samples' properties. For standard EC the electrical properties of a sample are recorded as variations in the complex impedance plane of the transmitting coil, caused by variations in the dispersion of the magnetic field and electrical circular currents in the sample. An electronic oscillator generates an alternating current that passes through a transmitting coil and causes a primary magnetic field B with magnetic flux Φ_B which is given in Equation (1). When Φ_B changes because B changes, Faraday's law states that the electromotive force is acquired, which is given in Equation (2) as U_{ind} [21–24].

$$\nabla \times E = -\frac{\partial B}{\partial t} \tag{1}$$

$$U_{ind} = -\frac{\partial \Phi_B}{\partial t} \tag{2}$$

When the conductive sample is placed in the impact zone of the coil, eddy currents J and displacement currents J_D are generated in the sample (Equation (3)) causing the secondary magnetic field to try and counteract the primary magnetic field and change it. Whereas the higher the frequency of excitation the stronger are the displacement currents expressed [24]. The ability of HF EC to excite the displacement currents shows its advantage over a standard Eddy Current (EC).

$$\nabla \times H = J + J_D \tag{3}$$

The measured difference of induced voltage is thereafter represented in the complex impedance plane as real and imaginary parts. Whereby, the real part corresponds to the active resistance R and the imaginary part expresses reactance X of the material. The impedance Z is calculated as given in Equation (4):

$$Z = \sqrt{R^2 + X^2} \tag{4}$$

Figure 1 illustrates how change of resistance and reactance of the material shifts the work point obtained by EC measurements in the complex impedance plane from Z_1 to Z_2. This effect can be used for monitoring the change of the material properties as a function of time.

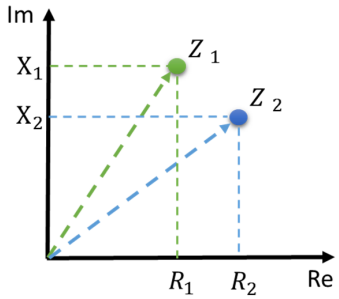

Figure 1. Work point in the complex impedance plane.

2.2. Particle Based Films

Particle based films consist of a carrier matrix and a filling material in the form of particles. The type of the film, dielectric or electrical, is defined by the type and concentration of particles in a carrying matrix. In this work films based on conductive particles are considered. In this case, it should be considered that their electrical resistance changes during drying [25–28]. Figure 2 demonstrates schematically the drying process of particle based films.

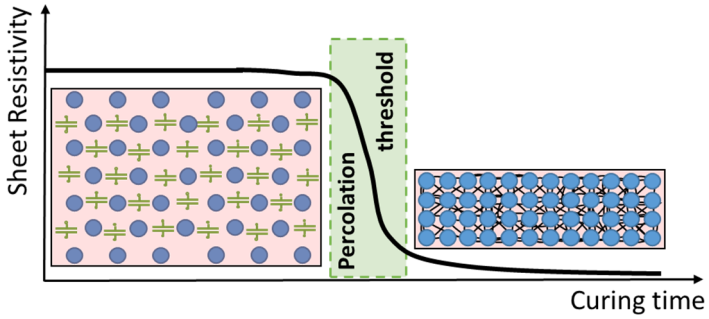

Figure 2. Curing process of particle based films.

After deposition, the distance between particles is large due to the presence of the chemicals used to make possible the mixing together of particles and epoxy. The electrical resistance is high. This is represented in Figure 2 as the amount of capacitors between particles before the percolation threshold. We represented the capacitors to show that before the percolation threshold, the dielectric properties of particles change when the electro-magnetic field is applied, due to polymerization and permittivity changes. During drying, chemicals evaporate and particles become closer to each other, whereas the film shrinks. When particles are in contact with each other the film's conductivity appears. The time at which this effect occurs is called the percolation threshold [29]. After the percolation threshold is reached the thickness does not change anymore and the polymerization process of the epoxy has started.

To enable monitoring of the overall drying process of particle based films a method allowing the measurements of not only electrical (electrical resistance) but also dielectric (capacitance) properties should be selected, which is possible by the HFEC method proposed in this work.

2.3. Sample Preparation

Particle based films were mixed at room temperature and under normal conditions. First, the polymer resin and the hardener were mixed together in the mass ratio of 4:1 respectively according to the specification. Thereafter the coupling and the solvent agent were added and the mixture was stirred for 10 min to blend. After adding conductive particles, the mixture was mixed for a further 10 min. Table 1 provides information about the composition of particle based films.

Table 1. Composition of particle based films.

Filling Material	Conductive Particles
Weight percentage wt.%	70%
Polymer matrix	2-Component Epotek 301
Coupling agent	3-Glycidoxypropyltrimethoxy silane
Solvent agent	Alcohol 94% and n-butyl acetate 99%

The epoxy system ensures a total drying time of the particle based films of 24 h at room temperature. The solvent is well dissolved with this type of epoxy and evaporates before the polymer

matrix polymerization begins. The coupling agent is added to the mixture to improve the particle dispersion in the matrix adhesive [30].

After preparation, wet conductive coatings were deposited onto the substrate using the frame printing technique [31] by varying the next parameter: Type of conductive particles, the thickness of the frame, the coated area, and the type of substrate (Figure 3).

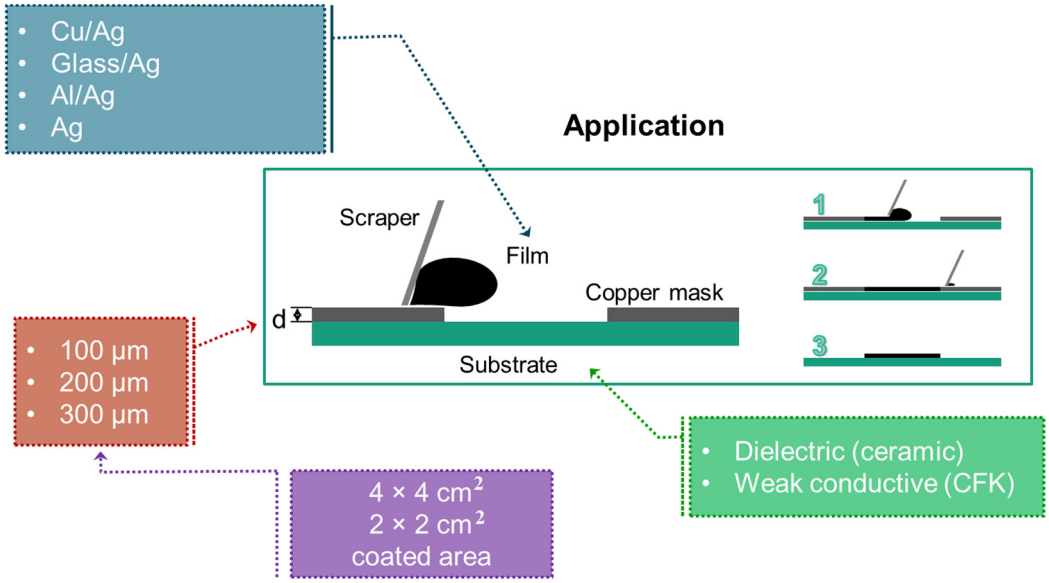

Figure 3. Schematic of the frame printing technique.

Four types of particles were used in this work and are listed in Table 2 below. The Cu/Ag particle provide the lowest resistance of the film after drying and the glass/Ag particle provide the highest resistance.

Table 2. Conductive particles specification.

Name	Average Size, µm	Ag Metal, wt.%
Silver coated copper (Cu/Ag) SC05F15 (Potters)	15	30–13
Silver coated glass (Glass/Ag) SG05TF40 (Potters)	35	23
Silver coated aluminum (Al/Ag) SA300S20 (Potters)	20	40
Silver (Ag) (Sigma-Aldrich, Darmstadt, Germany)	99.9	10

Three masks were used for films deposition having a thickness of 100, 200, and 300 µm. The initial thickness of the deposited films depends on the mask thickness and reduces during drying because of shrinkage. Each used copper frame has a rectangular opening of 40 mm × 40 mm and 20 mm × 20 mm, etched in the center; with this, the coated area is provided. Varying the coated area is especially important for HFEC measurements to investigate the influence of the edge effects on the measurements.

Two types of substrates were used in this work:

- Ceramic Al_2O_3: Length 68 mm, width 68 mm, thickness 0.63 mm;
- CFRP: Length 68 mm, width 68 mm, thickness 5 mm.

Ceramic substrate is used as it does not have its own conductivity and the HFEC measurements are influenced only by the changes in particle based films. Knowing the drying behavior of the particle based films on a ceramic substrate, the influence of the CFRP substrate on HFEC measurements can be estimated.

2.4. HFEC Measurements on Particle Based Films

After deposition, the particle based films are placed within a range of HFEC emission and measurements start immediately. The distance between the sensor and the film is 100 µm and measurements are performed at 30 s intervals over 24 h (from the beginning to the end of the drying).

The HFEC system used for the measurements is shown in Figure 4. It consists of a Laptop with installed software EddyWet 2.0 (Fraunhofer IKTS, Dresden, Germany), electronics, and sensor with two axial coils (Figure 4a). The sensor-box is shown in Figure 4b. The transmission coil is wound inside the ferrite cap and the pick-up coil outside of the cap so that the electromagnetic flux does not influence directly the pick-up coil (Figure 4c). The preamplifier is located close to the coil inside the sensor-box (Figure 4d) to stabilize the signal and to reduce the parasitic effects of stray fields and similar effects.

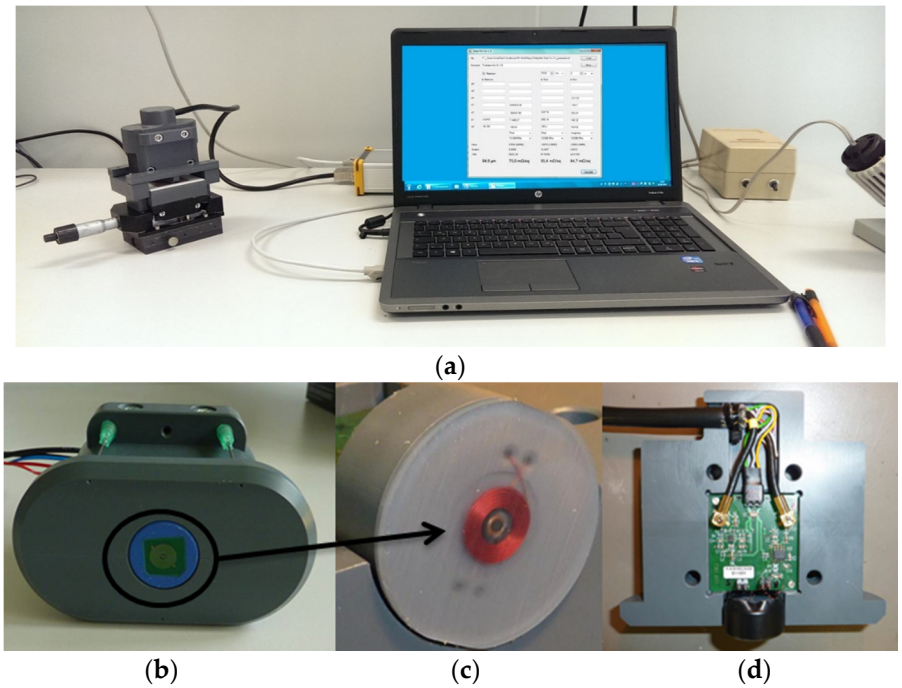

(**a**)

(**b**) (**c**) (**d**)

Figure 4. Photographs of the high-frequency eddy current (HFEC) system based on the EddyCus® System (**a**); sensor-box (**b**); coils configuration (**c**); and preamplifier inside of the sensor-box (**d**).

2.5. Reference Measurements

Due to the manual application process, the thickness of the coatings deviates from the desired value. Therefore, additional measurements on the films, called the reference, were performed and used by the analysis.

The electrical resistance of the dried samples was measured by the four-point probe method in the center of each coating using the multimeter consisting of a 2182A nanovoltmeter and 6221 DC and AC current source. In accordance with the geometry of the coated area and distance between the electrodes, the sheet resistivity, which is commonly used to characterize thin films [32], R_S is calculated as given by Equation (5) [33]:

$$R_S = \frac{V}{I} \times C \tag{5}$$

where V/I is a measured value, C is the correction factor for various geometries $C(\frac{a}{d};\frac{d}{s})$. Figure 5 shows parameters a, d, and s for a rectangular geometry.

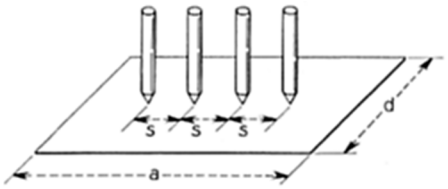

Figure 5. Four-point probe method.

In this particular case s = 2 mm. This gives a correction factor for 4 cm × 4 cm geometry c = 4.4516 and for the geometry of 2 cm × 2 cm c = 4.2209.

The thickness of the film d (in cm) and its electrical resistance ρ (in Ω·cm) are related to the calculated R_s as given by Equation (6):

$$R_S = \frac{\rho}{d} \quad (6)$$

In the literature, the units of R_s are ohm per square or Ω/sq. which is given on the graphs (Figures 8–16) as Ω/□ [32].

3. Results

3.1. Experimental Results of HFEC Measurements on Particle Based Films

3.1.1. Curing Process Comparison for Particle Based Films

The first part of the experiment was outlined to find out if and how the type of particles influences the drying process of the particle based films. The data obtained by HFEC measurements for particle based films are represented as real R_e(U) and imaginary I_m(U) parts in digits of the complex voltage as a function of the drying time. For offset compensation, the HFEC drying curves were normalized to a value that was measured in the first seconds of the drying period. Figure 6 shows schematically the drying process for all films deposited onto the ceramic substrate as a function of the real part of the drying time at a frequency of 10 MHz. The system resonance frequency is 11 MHz. The frequency of 10 MHz is located before the resonance allowing the measuring of the maximal dielectrically changes in the film and was therefore selected for this analysis.

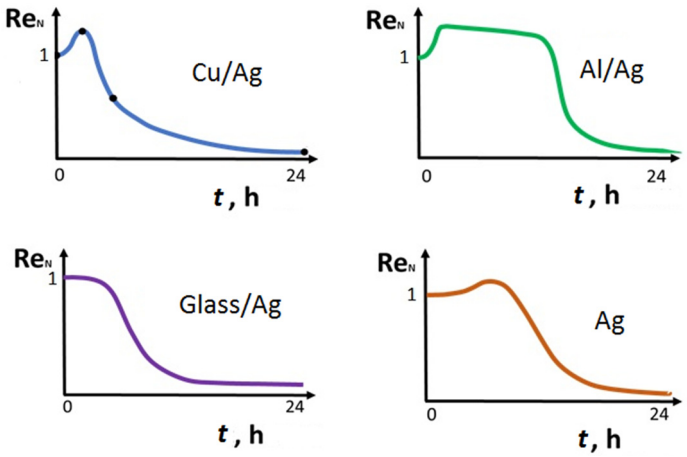

Figure 6. Normalized "real part" amplitude dependence on the cure time for 4 types of coatings at a frequency of 10 MHz.

It can be seen from Figure 6 that three of the measured films have a signal amplitude that increases (peak on the graphs) that was deducted and called "the characteristic point" but is expressed in different ways depending on the different coatings type. For glass/Ag films no characteristic point

can be detected. Because only the type of particles was varied, we assume that the conductivity of the conductive particles influences strongly the capacitive effects while their percolation threshold, which affects the HFEC measurements reacting on the dielectric properties, changes. The glass/Ag films provide the highest final sheet resistivity and therefore the lowest final conductivity, which leads to capacitive effects during the percolation not being strongly expressed. Thus it became clear that, the type of particles influences dramatically the drying process of particle based films and it is possible to monitor and to visualize it by HFEC.

3.1.2. Reference Measurements

References proving information about the final sheet resistivity of the particle based films are given in Tables 3–6 below.

Table 3. Cu/Ag films on ceramic substrate with coated area of 4 cm × 4 cm.

Screen Printing Frame Thickness	Final Sheet Resistivity of the Conductive Coatings
Thin d = 100 µm	R_{S1-1} = 71.67–138 mΩ/sq.
Middle d = 200 µm	R_{S1-2} = 28.05–43.18 mΩ/sq.
Thick d = 300 µm	R_{S1-3} = 22.7–27.16 mΩ/sq.

Table 4. Glass/Ag films on ceramic substrate with coated area of 4 cm × 4 cm.

Screen Printing Frame Thickness	Final Sheet Resistivity of the Conductive Coatings
Thin d = 100 µm	R_{S2-1} = 436.3–934.8 mΩ/sq.
Middle d = 200 µm	R_{S2-3} = 287.6–338.3 mΩ/sq.
Thick d = 300 µm	R_{S2-3} = 164.7–267.1 mΩ/sq.

Table 5. Cu/Ag films on ceramic substrate with coated area of 2 cm × 2 cm.

Screen Printing Frame Thickness	Final Sheet Resistivity of the Conductive Coatings
Thin d = 100 µm	R_{S3-1} = 51.9–65.4 mΩ/sq.
Middle d = 200 µm	R_{S3-2} = 45.6–57.8 mΩ/sq.
Thick d = 300 µm	R_{S3-3} = 30.8–32.1 mΩ/sq.

Table 6. Cu/Ag films on CFRP substrate with coated area of 4 cm × 4 cm.

Screen Printing Frame Thickness	Final Sheet Resistivity of the Conductive Coatings
Thin d = 10 µm	R_{S4-1} = 67.7–89 mΩ/sq.
Middle d = 200 µm	R_{S4-2} = 40.1–54.8 mΩ/sq.
Thick d = 300 µm	R_{S4-3} = 26.7–44.5 mΩ/sq.

Films deposited using the thin frame are colored with a blue line or point in Figures 7–16, for the middle frame a green color is used and a red for films deposited through the thick frame. The measured values of the sheet resistivity deviate from the desired value due to the hand process of deposition. Next cross-correlations in Section 3.2.2 shows that even if the desired value was not reached, HFEC measurements indicate it.

3.1.3. Amplitude Dependence on the Curing Time for Cu/Ag and Glass/Ag Films with Coated Area of 4 cm × 4 cm on Ceramic Substrate

Two of the films were chosen for performing further analysis: Cu/Ag and glass/Ag films. Both films were selected in order to investigate two cases: with and without a "characteristic point" and to find out if the films could be characterized in a wet state. Now not only the type of particles was considered but the thickness of the film as well.

Figure 7 illustrates HFEC measurement results for thin, middle, and thick Cu/Ag and glass/Ag films by representing the normalized amplitude of the real part as a function of the drying time in min (logarithmic scale). It is seen that there are three main parts during drying marked in Figure 7 as states (1), (2) and (3). These three states are a particular development of this work. The time of each corresponding state (1), (2) and (3) depends on the chemical composition, environmental conditions, curing temperature, thickness of the film, coated area etc. For films monitored in this study, these three states were evaluated as average times: state (1)—30 min, state (2)—70 min, state (3)—24 h.

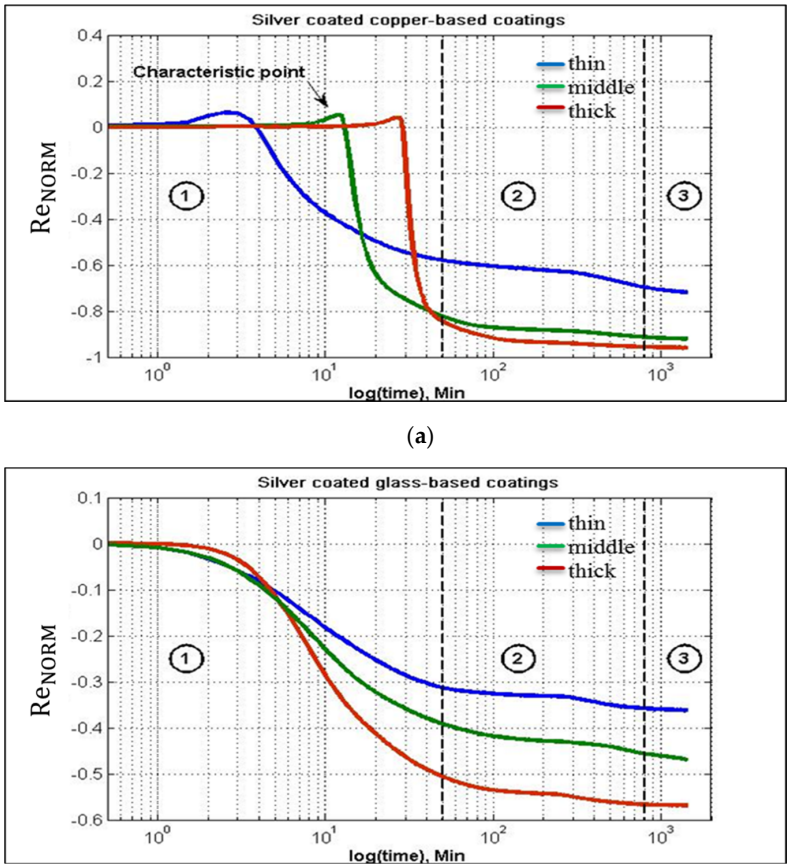

Figure 7. Experimental results of the HFEC measurements on Cu/Ag (**a**) and glass/Ag (**b**) films at a frequency of 10 MHz.

State (1) characterizes the percolation processes in the film [20] which occur because of the evaporation of chemicals and decreasing film thickness. State (2) shows the polymerization of the film, and state (3) corresponds to the end of the curing. It was deduced by measurements in this work data that "the characteristic" point provides correlations between the measured amplitude of the real part and final sheet resistivity. Correlations for glass/Ag films are not possible in this state. However, correlations in states (2) and (3) are possible for both Cu/Ag and glass/Ag films.

Figure 8 shows a correlation between the final sheet resistivity and the amplitude of the real part expressed in digits measured by HFEC spectroscopy for Cu/Ag films with different thicknesses at the "characteristic point" at a frequency of 10 MHz. The final sheet resistivity is taken from Tables 3 and 4 for Cu/Ag and glass/Ag particles respectively.

In Figures 8–16 the color illustrates which frame was used by films deposition (thin, middle or thick). However, it should be noted that the desired values were not reached, defects in the film thickness occurred during deposition, influencing their final sheet resistivity. Thus, the color shows

the desired value, and the final resistivity on the x-axis in the graphs shows the measured, actual sheet resistivity. For convenience, films in Table 3 are marked with triangles, in Table 4 with circles, in Table 5 with rhombuses and in Table 6 with quadrats.

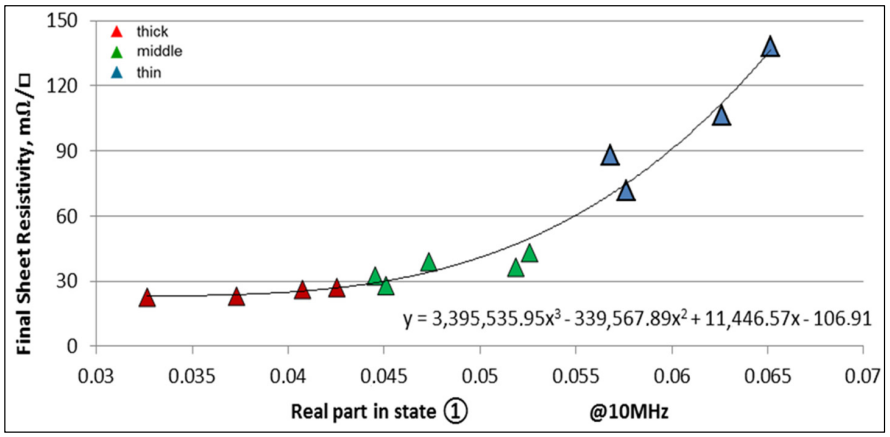

Figure 8. Correlations between the final sheet resistivity and the real part in state (1) at a frequency of 10 MHz for Cu/Ag films.

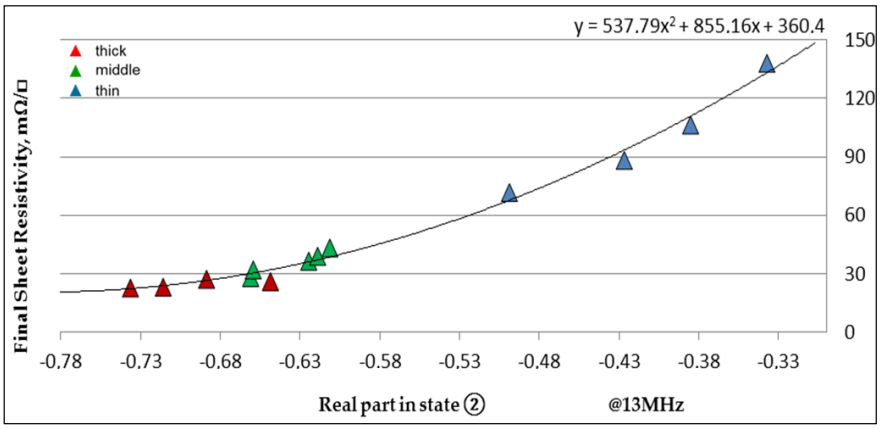

Figure 9. Correlations between the final sheet resistivity and the real part in state (2) at a frequency of 13 MHz for Cu/Ag films.

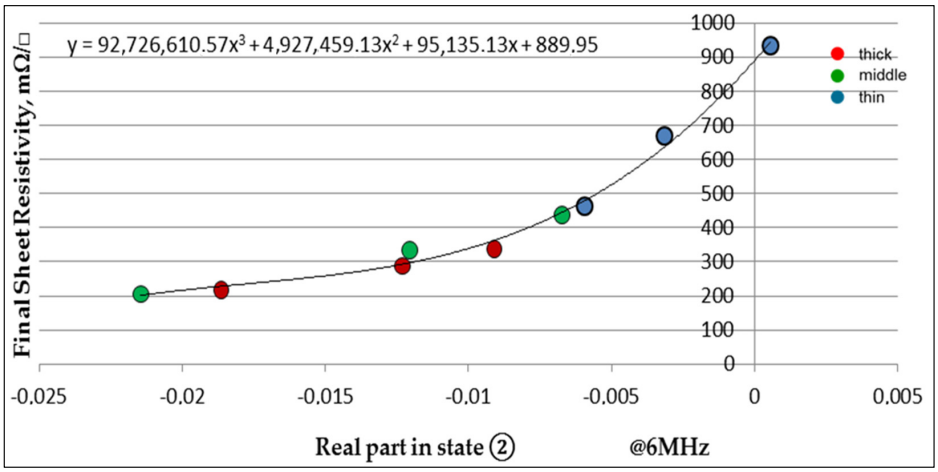

Figure 10. Correlations between the final sheet resistivity and the real part in state (2) at a frequency of 6 MHz for glass/Ag films.

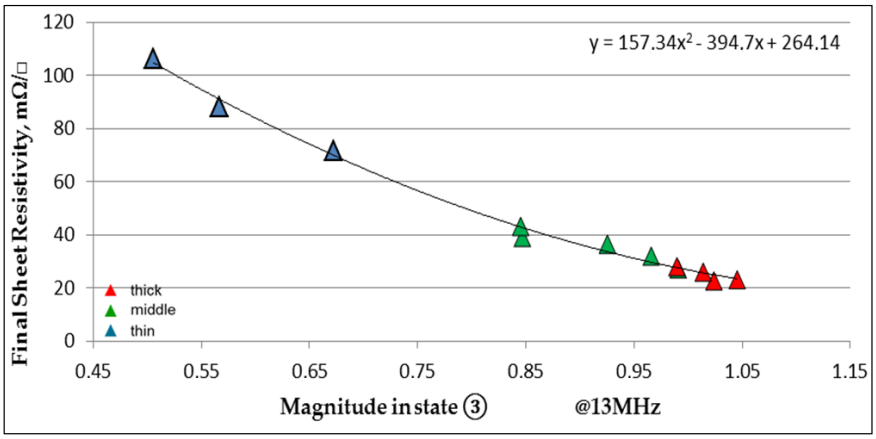

Figure 11. Correlations between the final sheet resistivity and the magnitude in state (3) at a frequency of 13 MHz for Cu/Ag films.

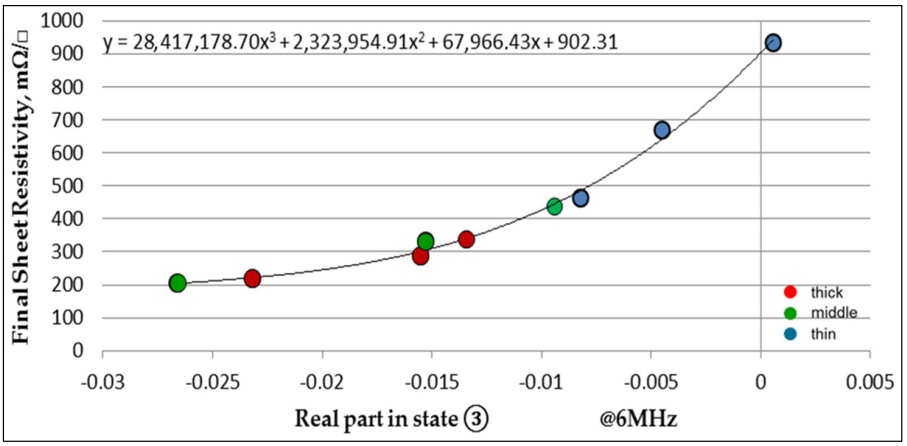

Figure 12. Correlations between the final sheet resistivity and real part in state (3) at a frequency of 6 MHz for glass/Ag films.

For both Cu/Ag and glass/Ag correlations in state (2) are possible, this occurs after 70 min for films produced in this work. The difference is that, for different films different frequencies for analyzing should be used. We assume that this is due to the conductivity of the particles. It was also experimentally established, that not only one parameter of HFEC provides correlation, such as the real part, but also the imaginary part and magnitude, which are given in this work as normalized values, namely each measured value is divided by the very first measured value. Figures 9 and 10 illustrate some of the possible correlations for Cu/Ag and glass/Ag films in state (2).

After the drying process has finished, correlation for both Cu/Ag and glass/Ag films are possible. Moreover, a number of frequencies can be used for characterization. For Cu/Ag films 6 MHz, 10 MHz, and 13 MHz are suitable and all HFEC parameters provide correlation: real and imaginary parts and magnitude as well. This allows characterization of different films in the same graph when required. Figures 11 and 12 show the most accurate correlation in state (3).

Thus, it can be seen from Figures 8–12, the correlations for both Cu/Ag and glass/Ag films are possible for the overall drying process. Final sheet resistivity and drying behavior in state (1) depends on the type of particles; the duration of each state, and the time when the "characteristic point" occurs, depending on the type of the polymer matrix and solvent agent. The type of polymer matrix and solvent agent prescribe the particle based films drying conditions and time. There are some frequencies for each film to be used for analyzing, these frequencies are located around the resonance frequency of the system. Creating a trend line through the measured points at different drying stages allows

the prediction of the film's final sheet resistivity overall drying process. This is an approach for in-situ monitoring for the particle based films drying process.

3.1.4. Amplitude Dependence on the Curing time for Cu/Ag Films with Coated Area of 2 cm × 2 cm on Ceramic and 4 cm × 4 cm on CFRP Substrates

As discussed in Section 2.3, films based on Cu/Ag particles are used for further investigation of the influence of the coated area and type of the substrate on the HFEC measurements. It can be deduced that there is no correlation for Cu/Ag films on CFRP substrate in state (1) which is due to the fact that CFRP is a conductive material. At the beginning of the drying process, mainly the dielectric properties changes occasion generation of HFECs and these changes are measured. In the case of CFRP, these effects can be dampened by the CFRP conductivity, and shift the amplitude and time of the "characteristic point". For Cu/Ag films with a coated area of 2 cm × 2 cm the "characteristic point" is observed as well, but only the time when the "characteristic point" occurs provides correlations. This states, that edge effects take place by HFEC measurement which should be taken into account when monitoring films on the structure boundaries. In states (2) and (3) correlations are possible for both Cu/Ag films with a coated area of 2 cm × 2 cm and on CFRP substrate. Figures 13–16 illustrate some correlations for these two cases. The final sheet resistivity is taken from Tables 5 and 6 for Cu/Ag based films deposited with a coated area of 2 cm × 2 cm on a ceramic substrate and with a coated area of 4 cm × 4 cm on the CFRP substrate respectively.

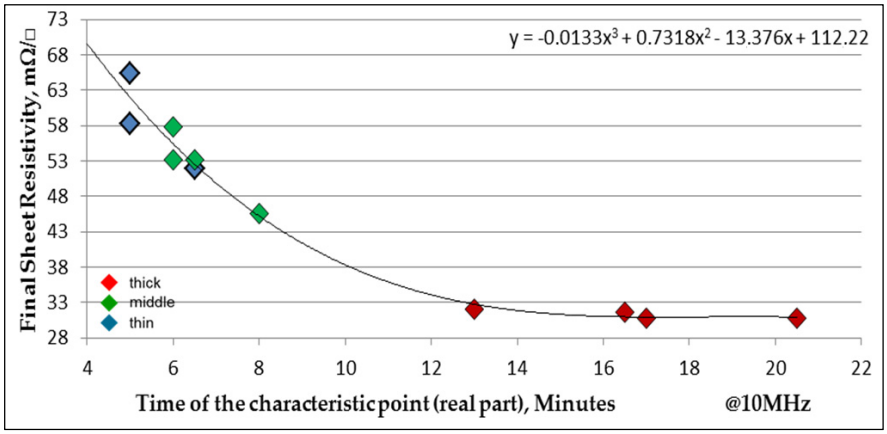

Figure 13. Correlations between the final sheet resistivity and the time of characteristic point at a frequency of 10 MHz for Cu/Ag films on ceramic substrate with coated area of 2 cm × 2 cm.

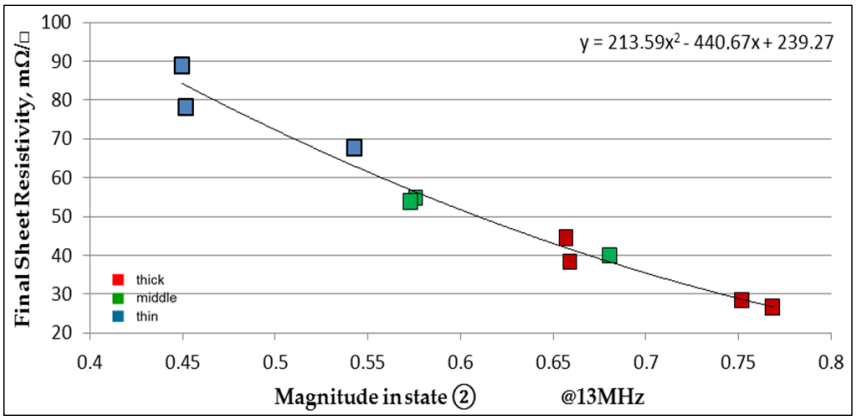

Figure 14. Correlations between the final sheet resistivity and the magnitude in state (2) at a frequency of 13 MHz for Cu/Ag films on CFRP substrate with coated area of 4 cm × 4 cm.

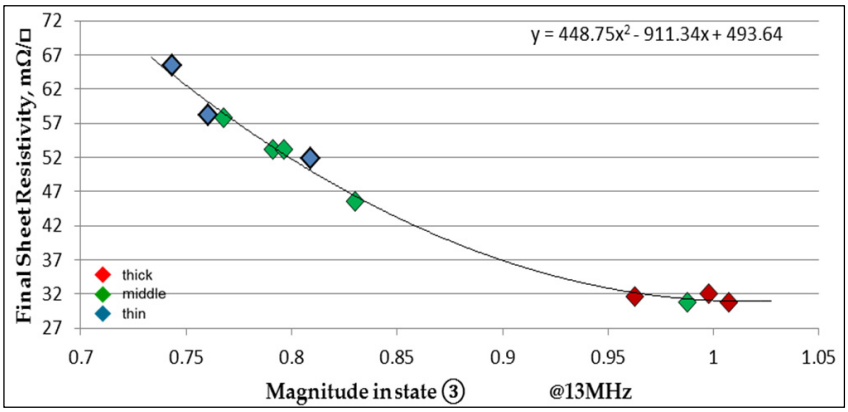

Figure 15. Correlations between the final sheet resistivity and the magnitude in state (3) at a frequency of 13 MHz for Cu/Ag films on ceramic substrate with coated area of 2 cm × 2 cm.

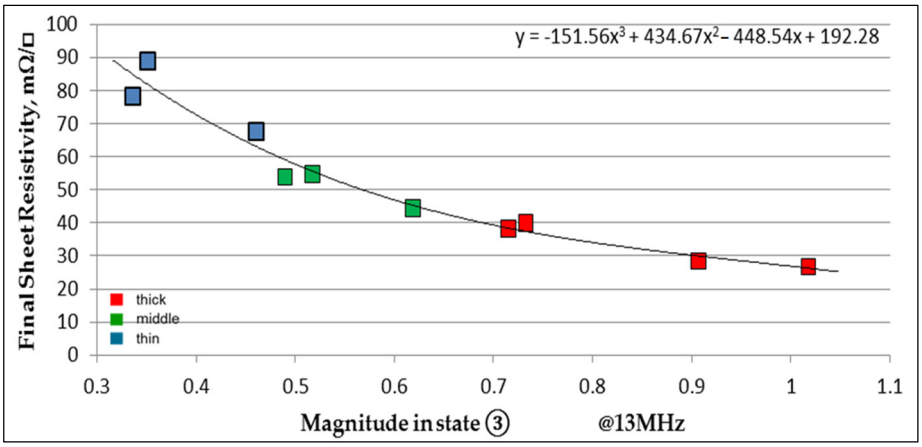

Figure 16. Correlations between the final sheet resistivity and the magnitude in state (3) at a frequency of 13 MHz for Cu/Ag films on CFRP substrate with coated area of 4 cm × 4 cm.

Similar to Cu/Ag and glass/Ag films with coated area of 4 cm × 4 cm on the ceramic substrate the trend lines created through measured points can be described by a polynomial function and used for the prediction of the film's final parameter at a different stage of drying. This was taken as a basis for the developed algorithm that is integrated in the HFEC based system together with software for this.

3.2. Software and HF EC System Dedicated Analysis of Particle Based Films Development

3.2.1. Software

A dedicated software named "Eddy Wet" (2.0) was developed to provide HF EC software for experiments to permit measurements in defined time steps over a longer curing time span. The following Figure 17 shows a screenshot of the "Eddy Wet" software interface.

The Software has the following options:

- Creates Frequency sweeps of a maximum of 245 frequencies;
- For each frequency, the matching gain is allocated;
- Time step of the measurements can be defined;
- When "Start" is pressed, HFEC starts a sweep and saves results and all parameters in a data file. HFEC continues the sweep after each time step, and saves the data (results) in the same data file;

- Data recording stops, when "Stop" is pressed;
- Between single sweep measurements HFEC excitation will not run, to prevent heating the coil and the sample;
- In the event of a system failure during the total drying time, the system saves the data file automatically and all data until the failures are eliminated;
- Resistivity button comprising an algorithm, is described in the following text.

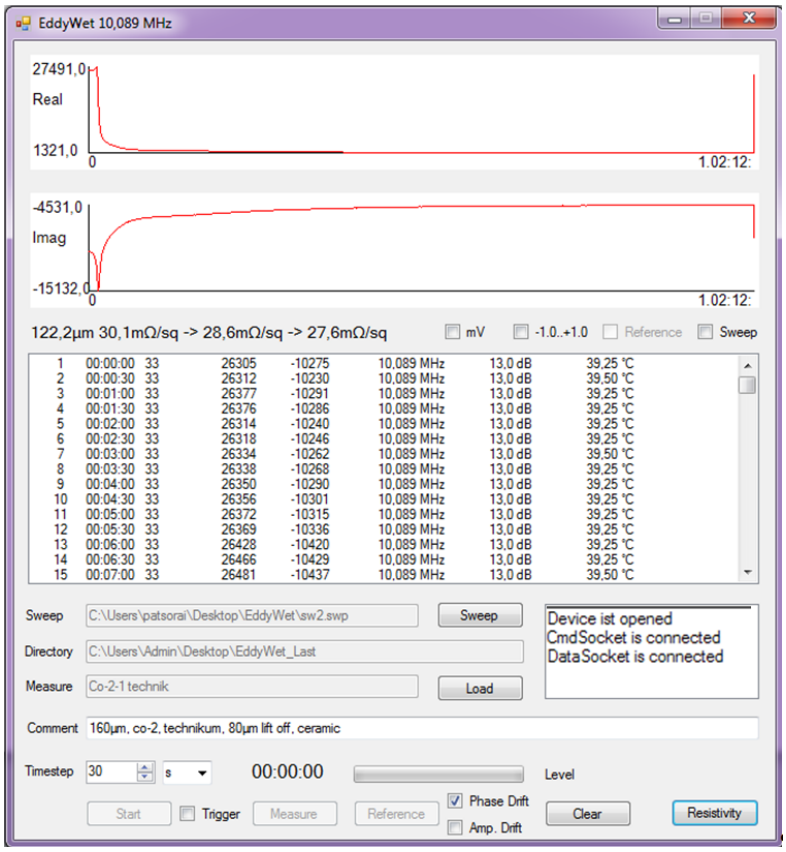

Figure 17. Screenshot of the "Eddy Wet" Main Menu.

Based on the correlations described in Section 3.1. An algorithm is developed. The principle of the algorithm can be described as follows. There are three states during curing—state (1) (percolation threshold, film is liquid), state (2) (polymerization process, film is wet), and state (3) (end of the drying, film is dried) for next wet conductive particle based:

- Cu/Ag films with coated area of 4 cm × 4 cm on ceramic substrate;
- Cu/Ag films with coated area of 4 cm × 4 cm on CFRP substrate;
- Cu/Ag films with coated area of 2 cm × 2 cm on ceramic substrate;
- Glass/Ag films with coated area of 4 cm × 4 cm on a ceramic substrate.

It can be seen from Figures 8–17 that each existing correlation has a trend line, which is defined by polynomial functions and can be generalized as shows Equation (7):

$$f(d,\sigma) = a_5x^5 + a_4x^4 + a_3x^3 + a_2x^2 + a_1x + a_0 \quad (7)$$

Using these coefficients, calibrations for new measurements can be created by using the "Resistivity" menu on the software panel (Figure 18). Calibration is used in the software to prescribe to the measured value of HFEC the predicted value of the final sheet resistivity of the film.

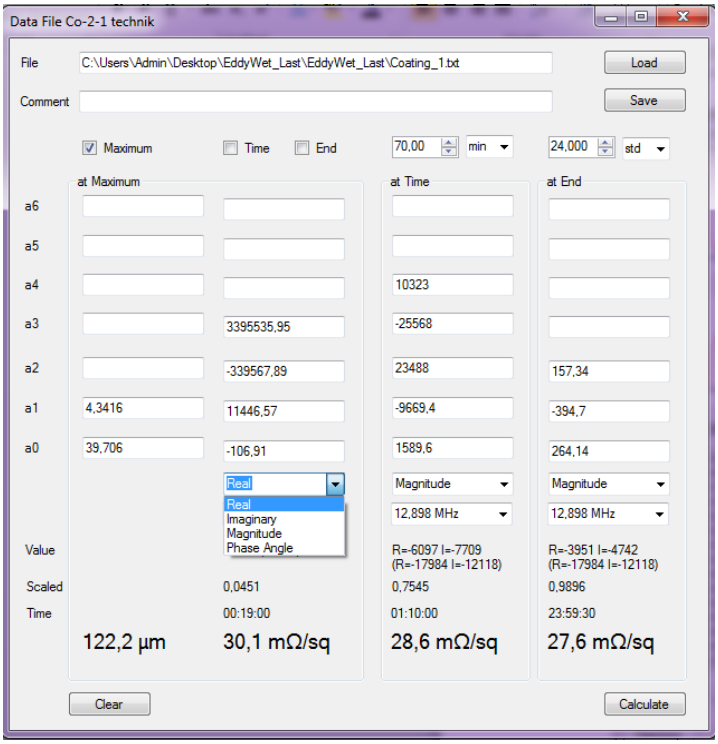

Figure 18. Screenshot of the "Resistivity" menu.

In the "Resistivity" window as shown in Figure 18 calibration curves can be prescribed for state (1) (at Maximum), state (2) (at Time), and state (3) (at End) by changing the coefficients "a_n". Because different films have different optimal frequencies for the prediction of their final parameters, the interface of the "Resistivity" menu includes an option for selecting the frequency for each state as well as the HFEC parameter that should be analyzed (real, imaginary parts, phase or magnitude.). After adding all coefficients, the file should be saved and can be used for calibration by the next measurements. When the "Resistivity" file is saved, by running measurements, as soon as the states (1), (2) and (3) occur, the final resistivity will be shown in the Eddy Wet main menu (Figure 19). The red arrow in Figure 19 indicates predicted values of the final sheet resistivity of the Cu/Ag film during drying. After the maximum of the amplitude of the real part was reached, the predicted value of the final sheet resistivity was 30.1 mΩ/sq. After 70 min passed, this predicted value became 28.6 mΩ/sq and after 24 h the predicted sheet resistivity was 27.6 mΩ/sq. The actual value of the sheet resistivity of this film was measured by a four-point probe method after drying and it is 27.16 mΩ/sq.

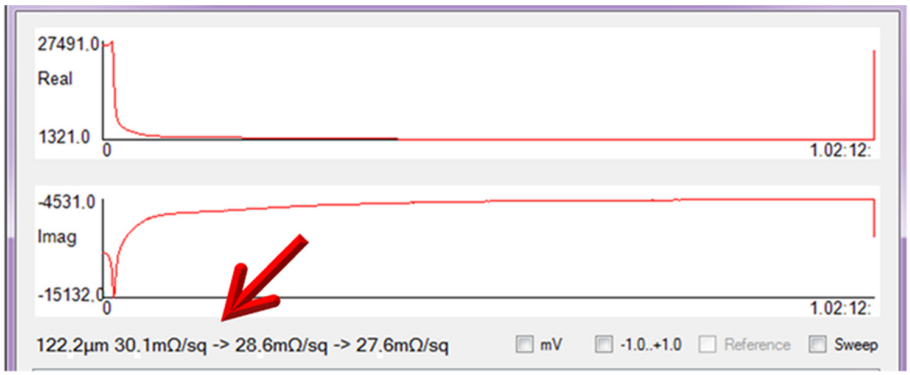

Figure 19. Screenshot of the Eddy Wet main menu illustrating prediction of the final parameter of particle based film.

3.2.2. HFEC System for Special Analyzing of Particle Based Films

The developed HFEC System based on the EddyCus® System designed and manufactured by Fraunhofer IKTS is a labor prototype and consists of 2 HFEC sensors, electronics, PC, and software for data analysis and visualization (Figure 20).

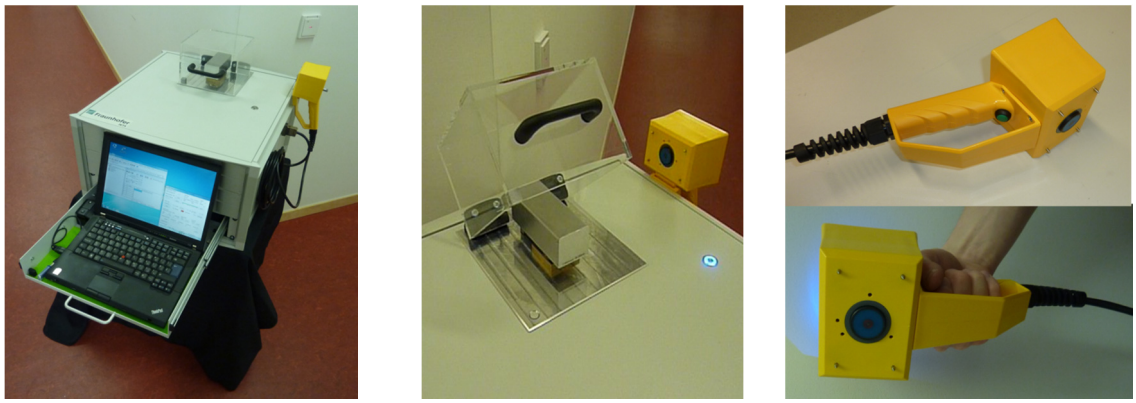

(**a**) (**b**) (**c**)

Figure 20. Photo of the HFEC System for special analysis of particle based films. System (**a**), view HFEC sensor for laboratory long time measurements (**b**), view handheld HFEC sensor (**c**).

The PC is located in a rack enclosure and can be pulled out. The system includes two types of sensors. One of the two sensor systems for laboratory long time measurements is located at the top of the box. Figure 20b shows this EC sensor, a sample holder, and a movable z-axis for varying the distance between sensor and sample. This sensor can be used for measurements of wet coatings on flat samples under lab conditions; for example, to record data for calibration curves. The second sensor (Figure 20c), including a similar coil, is located in a handheld sensor, which can be manually applied. This sensor has four needles (stand-off) that contact the structure to achieve a constant distance between the coil and the sample. The length of the needles can be adjusted using a precision positioning plate, which is integrated into the sensor; the setup button is located on the bottom of the sensor. In addition, the sensor has a release on the handheld sensor.

4. Conclusions

Results of this work show that it is possible to analyze and to monitor the overall drying process of particle based films by using HFEC spectroscopy. Based on results it is possible to state that films based on different particles and deposited with a different coated area or on the conductive substrate providing their own drying behavior, can be monitored in the wet state as well as after the drying process has finished. The HFEC reacts to the smallest changes in the film. This is an approach not only to monitor films resistivity in-situ but also to manufacture films with predetermined properties, which would be relatively easily accessed by HFEC or to control which type of particles could be used in films as well as to determine the quality of the particles or even the age of the coating. Another approach would be also the usage of HFEC spectroscopy to monitor nanosized particle based films drying behaviors. This would require additional experiments to be performed.

Based on the results, an algorithm was developed and described in this paper allowing the prediction of the final parameters of particle based films in a wet state. An HFEC testing system for special issues in surface analysis was developed. The system is comprised of two special HFEC sensors, PC, electronics, and software based on a multi-frequency algorithm.

The next step is aligned to develop a mathematical model allowing description of the processes occurring during drying in particle based films even without performing supplementary references.

Acknowledgments: We acknowledge support by the German Research Foundation and the Open Access Publication Fund of the TU Dresden.

Author Contributions: Henning Heuer provided the basic idea of monitoring the percolation process with HF eddy current and the equipment and staff Iryna Patsora and Susanne Hillmann conceived and designed the experiments, contributed reagents/materials/analysis tools. Iryna Patsora and Dmytro Tatarchuk developed an algorithm and wrote the MatLab script for data analyzing. Iryna Patsora performed the experiments and wrote the paper.

Conflicts of Interest: The authors declare no conflict of interest.

References

1. Electrically conductive adhesives. Available online: http://www.masterbond.com/properties/electrically-conductive-adhesive-systemsMaster. (accessed on 20 December 2016).
2. Lu, D.; Tong, Q.K.; Wong, C.P. Conductivity mechanisms of isotropic conductive adhesives (ICA's). *IEEE Trans. Electron. Packag. Manuf.* **1999**, *22*, 223–227.
3. Sancaktar, E.; Bai, L. Electrically Conductive Epoxy Adhesives. *Polymers* **2011**, *3*, 427–466. [CrossRef]
4. Szatkowski, G.N.; Nguyen, T.X.; Koppen, S.V.; Ely, J.J.; Mielnik, J.J. Electrical characterization of lightning strike protection techniques for composite materials. In Proceedings of 2009 International Conference on Lightning and Static Electricity (ICOLSE2009), Pittsfield, MA, USA, 15 September 2009.
5. Fan, L.; Tison, C.; Wong, C.P. Understanding of electrically conductive adhesives: Formulation, curing and conductivity. In Proceedings of the 8th International Advanced Packaging Materials Symposium, Stone Mountain, GA, USA, 3–6 March 2002.
6. Park, H.Y.; Jin, J.S.; Yim, S.; Oh, S.H.; Kang, P.H.; Choi, S.K.; Jang, S.Y. Effects of surface characteristics of dielectric layers on polymer thin-film transistors obtained by spray methods. *Phys. Chem. Chem. Phys.* **2013**, *15*, 3718–3724. [PubMed]
7. Mahan, J.E. *Physical Vapor Deposition of Thin Films*; Wiley: New York, NY, USA, 2000.
8. Lin, L.Y.; Lee, J.H.; Hong, C.E.; Yoo, G.H.; Advani, S.G. Preparation and characterization of layered silicate/glass fiber/epoxy hybrid nanocomposites via vacuum-assisted resin transfer molding (VARTM). *Compos. Sci. Technol.* **2006**, *66*, 2116–2125. [CrossRef]
9. Gay, D. *Composite Materials: Design and Applications*; CRC press: Boca Raton, FL, USA, 2014.
10. Gibson, R.F. A review of recent research on mechanics of multifunctional composite materials and structures. *Compos. Struct.* **2010**, *92*, 2793–2810. [CrossRef]
11. Gou, J.; Tang, Y.; Liang, F.; Zhao, Z.; Firsich, D.; Fielding, J. Carbon nanofiber paper for lightning strike protection of composite materials. *Compos. Part B Eng.* **2010**, *41*, 192–198. [CrossRef]
12. Eslamian, M.; Newton, J.E. Spray-on PEDOT:PSS and P3HT:PCBM Thin Films for Polymer Solar Cells. *Coatings* **2014**, *4*, 85–97. [CrossRef]
13. Fantino, E.; Chiappone, A.; Calignano, F.; Fontana, M.; Pirri, F.; Roppolo, I. In Situ Thermal Generation of Silver Nanoparticles in 3D Printed Polymeric Structures. *Materials* **2016**, *9*, 589. [CrossRef]
14. Larsson, A. The interaction between a lightning flash and an aircraft in flight. *Comptes Rendus Phys.* **2002**, *3*, 1423–1444. [CrossRef]
15. Gagné, M.; Therriault, D. Lightning strike protection of composites. *Prog. Aerosp. Sci.* **2014**, *64*, 1–16. [CrossRef]
16. Sharma, S.; Nivetha, A.; Maalavan, A.; Subramanian, K.S.; Kumar, S.S. Novel Lightning Strike-Protected Polymeric Composite for Future Generation Aviation. *J. Aerosp. Eng.* **2016**. [CrossRef]
17. Ha, M.S.; Kwon, O.Y.; Choi, H.S. Improved Electrical Conductivity of CFRP by Conductive Nano-Particles Coating for lightning Strike Protection. *J. Korean Soc. Compos. Mater.* **2010**, *23*, 31–36. [CrossRef]
18. Hillmann, S.; Heuer, H.; Calzada, J.; Cooney, A.; Foos, B.; Meyendorf, N. Characterization of wetconductive coatings using eddy current techniques. *AIP Conf. Proc.* **2012**, *1430*, 441–448.
19. Tsai, Y.J.; Chang, C.Y.; Lai, Y.C.; Yu, P.C.; Ahn, H. Realization of Metal Insulator Transition and Oxidation in Silver Nanowire Percolating Networks by Terahertz Reflection Spectroscopy. *ACS Appl. Mater. Interfaces* **2014**, *6*, 630–635. [CrossRef] [PubMed]
20. Zhang, P.; Santoro, G.; Yu, S.; Vayalil, S.K.; Bommel, S.; Roth, S.V. Manipulating the Assembly of Spray-Deposited Nanocolloids: In Situ Study and Monolayer Film Preparation. *Langmuir* **2016**, *32*, 4251–4258. [CrossRef] [PubMed]

21. Diggle, P.J. Overview of statistical methods for disease mapping and its relationship to cluster detection. *Spat. Epidemiol. Methods Appl.* **2000**. [CrossRef]
22. Dunnett, D.A. Classical Electrodynamics. *Nature* **1969**, *224*, 1334.
23. Jordan, E.C.; Balmain, K.G. *Electromagnetic Waves and Radiating Systems*; Prentice-Hall: Upper Saddle River, NJ, USA, 1968.
24. Stratton, J.A. *Electromagnetic Theory*; John Wiley & Sons: Chichester, UK, 2007.
25. Hillmann, S.; Heuer, H.; Meyendorf, N. High frequency eddy current device for near surface material characterizations. *Proc. SPIE Int. Soc. Opt. Eng.* **2009**, *7293*, 1–9.
26. Hillmann, S.; Klein, M.; Heuer, H. In-line thin film characterization using eddy current techniques. *Stud. Appl. Electromagn. Mech.* **2011**, *35*, 330–338.
27. Yating, Y.; Pingan, D.; Tuo, Y. Investigation on contribution of conductivity and permeability on electrical runout problem of eddy current displacement sensor. *IEEE* **2011**. [CrossRef]
28. Patsora, I.; Hillmann, S.; Heuer, H.; Foos, B.C.; Calzada, J.G. High-frequency eddy current based impedance spectroscopy for characterization of the percolation process of wet conductive coatings. *AIP Conf. Proc.* **2015**, *1650*, 414–423.
29. Essam, J.W. Percolation theory. *Rep. Prog. Phys.* **1980**, *43*, 7. [CrossRef]
30. Zhao, H.; Juang, T.; Liu, B. Synthetics and properties of copper conductive adhesives modified by SiO_2 nanoparticles. *Int. J. Adhes. Adhes.* **2007**, *27*, 429–433. [CrossRef]
31. Ito, S.; Chen, P.; Comte, P.; Nazeeruddin, M.K.; Liska, P.; Pechy, P.; Grätzel, M. Fabrication of screen-printing pastes from TiO_2 powders for dye-sensitised solar cells. *Prog. Photovolt. Res. Appl.* **2007**, *15*, 603–612. [CrossRef]
32. Van Zant, P. *Microchip Fabrication*; McGraw-Hill: New York, NY, USA, 2000.
33. Smits, F.M. Measurement of sheet resistivities with the four-point probe. *Bell Syst. Technol. J.* **1957**, *37*, 711–718. [CrossRef]